



# Comparison between $(\epsilon, \tau)$ entropy and sample entropy in a chaotic semiconductor laser

Tomohiko Okuma, Yu Kawaguchi, Kazutaka Kanno, and Atsushi Uchida

Department of Information and Computer Sciences, Saitama University,  
255 Shimo-Okubo, Sakura-ku, Saitama City, Saitama, 338-8570, Japan  
Emails: t.okuma.675@ms.saitama-u.ac.jp, auchida@mail.saitama-u.ac.jp

**Abstract** – The evaluation of unpredictability of chaotic laser outputs is important for the applications of physical random number generation. We evaluate the entropy rate of chaotic temporal waveforms generated from a semiconductor laser using the  $(\epsilon, \tau)$  entropy and the sample entropy in numerical simulations. We also calculate the Kolmogorov-Sinai entropy to show the validity of the entropy measurement.

## 1. Introduction

Random number generators are necessary for engineering applications, such as information security and numerical simulation. Pseudorandom number generators are based on deterministic algorithm, and they can generate fast random bit sequences. However, pseudorandom numbers are completely determined by a seed which is an initial value, and they have periodicity and reproducibility. On the contrary, physical random number generators are based on physical phenomena, and the sequences generated from physical random number generators are unpredictable and irreproducible. However, the speed of physical random number generators is relatively low.

To enhance the generation speed, physical random number generators based on chaotic semiconductor lasers have been proposed [1], where physical random number generation has been achieved at a rate of gigabit per second. Several post-processing methods have been reported to improve the randomness of generated bit sequences, such as least significant bit (LSB) extraction [2] and bit-order reversal [3]. Using these post-processing methods, the speed of random number generation based on chaotic semiconductor lasers can be improved at a rate up to terabit per second [4].

There is another issue that the speed of random number generation may exceed the rate of entropy (uncertainty) production in physical entropy sources. Therefore, it is necessary to evaluate the entropy generation rate of physical random number generators to ensure the generation of physical random bit sequences with unpredictability [5].

Kolmogorov-Sinai (KS) entropy is a standard measure of entropy in dynamical systems, and it is calculated from the sum of positive Lyapunov exponents [6]. It is necessary to use a numerical model to calculate the KS entropy, and

the KS entropy cannot be directly applied for the analysis of experimentally measured temporal waveforms generated from physical entropy sources.

The  $(\epsilon, \tau)$  entropy has been reported as a measure of entropy rate, which can be calculated from temporal waveforms [7,8]. The calculation of the  $(\epsilon, \tau)$  entropy is based on how many points exist in an  $\epsilon$ -size hypercube in a high dimensional attractor, which is reconstructed from the temporal waveforms sampled at the time interval  $\tau$  using time-delayed embedding. It has been known that the limit of the  $(\epsilon, \tau)$  entropy approaches the KS entropy ( $\epsilon \rightarrow 0, \tau \rightarrow 0$ ).

The sample entropy has also been reported as another measure of entropy rate, which can be directly calculated from temporal waveforms [9]. The sample entropy has been used in medical fields [10], and the validity of the sample entropy in chaotic semiconductor lasers has not been reported yet. The sample entropy is directly calculated from one-dimensional temporal waveforms, and the sample entropy can reduce the calculation time rather than the  $(\epsilon, \tau)$  entropy, which is calculated from a high-dimensional attractor.

In this study, we calculate the sample entropy from chaotic temporal waveforms in unidirectionally coupled semiconductor lasers, and compare the sample entropy with the  $(\epsilon, \tau)$  entropy in numerical simulations. We also calculate the KS entropy, which is estimated from the linearized equations of the numerical model, and show the validity of the estimation of the sample entropy and the  $(\epsilon, \tau)$  entropy by comparing with the KS entropy.

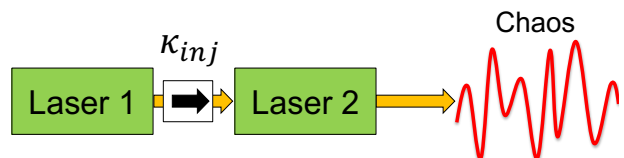


Fig. 1 Model for unidirectionally coupled two semiconductor lasers.

## 2. Numerical model of semiconductor lasers

In this section, we explain our numerical model of unidirectionally coupled semiconductor lasers. Figure 1 shows the model for unidirectionally coupled two semiconductor lasers. The optical output of the laser 1 is

injected into the laser 2. It has been known that the laser 2 can produce chaotic dynamics by adjusting the optical frequency detuning between the two lasers and the coupling strength of the optical injection signal from the laser 1 to 2.

The dynamics of the semiconductor laser is described by the Lang-Kobayashi equations [11]. The model of the laser 2 is described as follows,

$$\frac{dE_2(t)}{dt} = \frac{1 + i\alpha}{2} \left[ \frac{G_N(N_2(t) - N_0)}{1 + \epsilon|E_2(t)|^2} - \frac{1}{\tau_p} \right] E_2(t) + \kappa_{inj} E_1(t) \exp(i(\Delta\omega t - \omega_1 \tau_{inj})) \quad (1)$$

$$\frac{dN_2(t)}{dt} = J_2 - \frac{N_2(t)}{\tau_S} - \frac{G_N(N_2(t) - N_0)}{1 + \epsilon|E_2(t)|^2} |E_2(t)|^2 \quad (2)$$

Where  $E_2(t)$  is the complex electric field, and  $N_2(t)$  is the carrier density for the laser 2. The optical intensity  $I(t)$  and the optical phase  $\phi(t)$  are calculated from the complex electric field  $E(t) = E_{Re} + iE_{Im}$ , where  $I(t) = E_{Re}^2 + E_{Im}^2$  and  $\phi(t) = \arctan(E_{Im}/E_{Re})$ .  $G_N$  is the gain coefficient,  $\alpha$  is the linewidth enhancement factor,  $N_0$  is the carrier density at transparency,  $\gamma$  is the gain saturation coefficient,  $\tau_S$  is the carrier lifetime, and  $\tau_p$  is the photon lifetime.  $J_2$  is the injection current for the laser 2. We set  $J_2 = 1.36J_{th}$  where  $J_{th}$  is the injection current at the lasing threshold.  $E_1$  is the electric field amplitude of the laser 1.  $E_1$  is calculated from a steady-state solution of the Lang-Kobayashi equations without optical injection [12]. We set the initial optical frequency detuning ( $\Delta f = \Delta\omega/2\pi = (\omega_1 - \omega_2)/2\pi$ ) to 1.30 GHz, where  $\omega_1 = 1.226 \times 10^{15} \text{ s}^{-1}$ . The injection strength is varied to observe different temporal dynamics of the laser 2. The other parameter values are given in [12].

Figure 2 shows the numerical results of the temporal waveforms of the optical intensity  $I(t)$  calculated from Eqs. (1) and (2). A quasiperiodic oscillation is observed for  $\kappa_{inj} = 9.0 \text{ ns}^{-1}$  in Fig. 2(a). As  $\kappa_{inj}$  increased, a chaotic temporal waveform is obtained for  $\kappa_{inj} = 10.0 \text{ ns}^{-1}$ , as shown in Fig. 2(b).

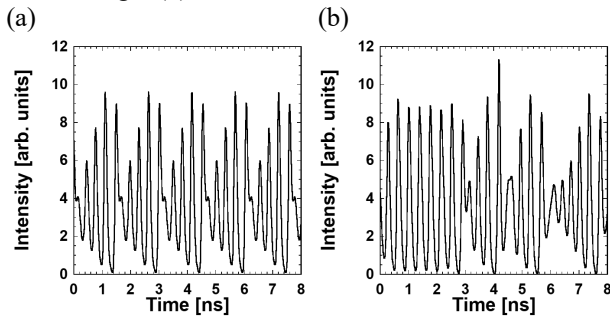


Figure 2: Numerical results of temporal waveforms of the laser intensity for different optical injection strengths  $\kappa_{inj}$ . (a)  $\kappa_{inj} = 9.0 \text{ ns}^{-1}$ , and (b)  $\kappa_{inj} = 10.0 \text{ ns}^{-1}$ .

To calculate the KS entropy, we derive the linearized equations from the original rate equations of Eqs. (1) and (2). We can calculate the Lyapunov spectrum from the

evolution of perturbations by integrating both the original and linearized equations. The KS entropy is calculated from the sum of positive Lyapunov exponents as follows [12],

$$h_{KS} = \sum_{i|\lambda_i > 0} \lambda_i \quad (3)$$

### 3. Calculation method of sample entropy

The dynamics of the laser 2 can be represented in three-dimensional phase space constructed from the optical intensity  $I(t)$ , the optical phase  $\Phi(t)$ , and the carrier density  $N(t)$  in the Lang-Kobayashi equations. In experiment,  $I(t)$  can be measured easily, whereas it is difficult to measure  $\Phi(t)$  and  $N(t)$  directly. Therefore, we calculate the sample entropy from the temporal waveforms of the optical intensity  $I(t)$ .

Figure 3 shows the concept of the calculation of the sample entropy. We use a chaotic temporal waveform of the optical intensity sampled at a sampling time interval  $\tau$ . The discrete time  $t$  is represented as  $i\tau$  ( $i = 1, 2, \dots, L$ , where  $L$  is the length of the temporal waveform). Next, we randomly select a point in the temporal waveform and prepare a reference vector  $\mathbf{X}_i$ . The reference vector  $\mathbf{X}_i$  is described as follows,

$$\mathbf{X}_i = [x(i\tau), x((i+1)\tau), \dots, x((i+d-1)\tau)] \quad (4)$$

We calculate the probability of the existence of the vectors which are similar to the reference vector  $\mathbf{X}_i$  in the temporal waveform. The probability is described as follows,

$$A_d = \log_2 \left( \frac{1}{R} \sum_{i=1}^R A_i \right) \quad (5)$$

where  $R$  is the number of the reference vector  $\mathbf{X}_i$ .  $A_i$  represents the probability of the existence of the vectors within the distance of  $\epsilon$  from the reference vector. The probability is averaged over  $R$  points. The reference vector  $\mathbf{X}_i$  is randomly selected for efficient calculations in this method. The entropy rate  $h_{samp}$  is calculated from  $A_d$  and  $A_{d+1}$  as follows,

$$h_{samp} = -\frac{1}{\tau} (A_{d+1} - A_d) \quad (6)$$

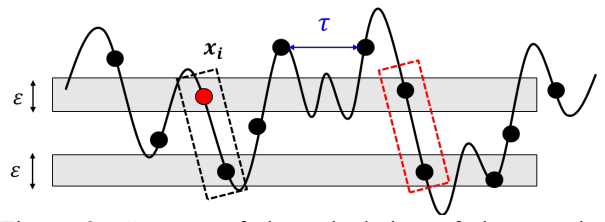


Figure 3: Concept of the calculation of the sample entropy from temporal waveforms.

Although the sample entropy is very similar to the  $(\epsilon, \tau)$  entropy, there are several differences between the two methods. First, the sample entropy is directly calculated from temporal waveforms, whereas the  $(\epsilon, \tau)$  entropy is calculated from vectors on a high-dimensional attractor reconstructed from temporal waveforms. Therefore, the calculation of the sample entropy is less time-consuming than that of the  $(\epsilon, \tau)$  entropy. In addition, the probability is averaged over the reference vectors first, and the natural logarithm of the averaged probability is calculated for the sample entropy. In contrast, the natural logarithm of the probability is calculated first, and the average is taken over the reference vectors for the  $(\epsilon, \tau)$  entropy. Also, the sample entropy does not include self-counting of the reference vector, while the  $(\epsilon, \tau)$  entropy includes self-counting of the reference vector to avoid the zero calculation of the natural logarithm of the probability.

We use the data length  $L$  of 1 Mega points, the number of reference points  $R$  of 5000 points, and the sampling interval  $\tau$  of 20 ps (50 GHz). We use  $\epsilon$  normalized by the standard deviation of temporal waveforms, because the standard deviation is changed for different dynamics and the amplitude of the temporal waveforms strongly affects the estimation of the entropy. We set  $\epsilon = \sigma 2^{\epsilon_s}$ , where  $\sigma$  is the standard deviation, and we change  $\epsilon_s$ .

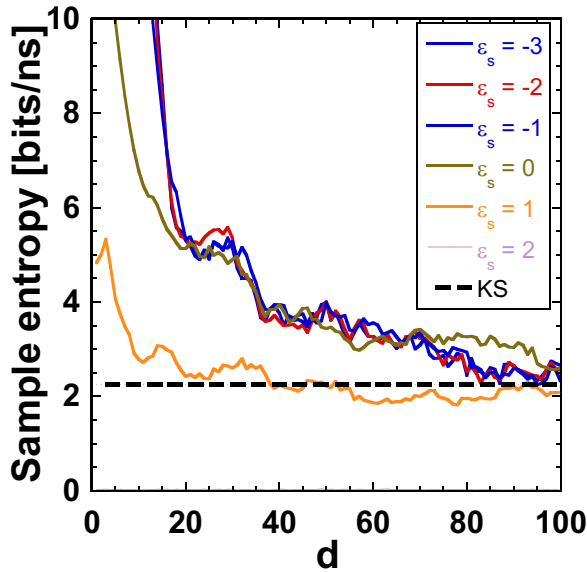


Figure 4: Numerical results of the sample entropy as a function of  $d$  for different  $\epsilon_s$ . The dotted line indicates the KS entropy.

#### 4. Numerical results of the sample entropy

For the calculation of the sample entropy, it is necessary to set appropriate values of  $\epsilon_s$ , and  $d$ . We investigate the dependence of the entropy on  $\epsilon_s$  and  $d$ . Figure 4 shows the sample entropy as a function of  $d$  for different  $\epsilon_s$ . For small  $d$ , a sufficiently long vector is not used from the temporal waveform, and the entropy is overestimated. For

large  $d$ , the entropy almost converges at a fixed value for small  $\epsilon_s$  and gradually approaches the value of the KS entropy (the dotted line in Fig. 4). Therefore, it is found that a large  $d$  and a small  $\epsilon_s$  are suitable for the evaluation of the sample entropy. We thus select the value of  $d = 100$  and  $\epsilon_s = 0$  for the evaluation of the sample entropy in Fig. 4.

#### 5. Comparison between the sample entropy and the KS entropy

To investigate the validity of the calculation of the sample entropy, we compare the sample entropy with the KS entropy. Figure 5(a) shows the sample entropy (the red curve) and the KS entropy (the black curve) as a function of the injection strength  $\kappa_{inj}$ . For comparison, the values of the sample entropy agree well with those of the KS entropy. Figure 5(b) shows the correlation plot between the sample entropy and the KS entropy, obtained from the data in Fig. 5(a). Very high correlation is obtained with the correlation value of 0.961. From these results, we confirm that the sample entropy matches the KS entropy well, and the sample entropy is a good measure for the entropy of chaotic temporal waveforms.

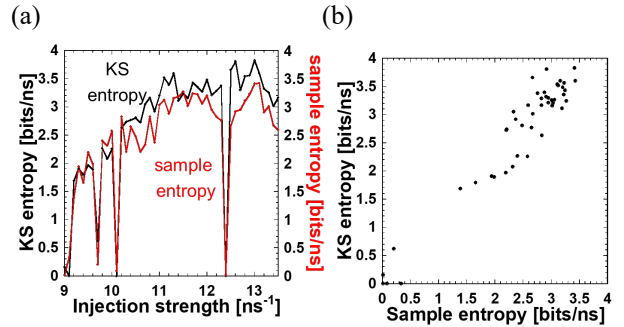


Figure 5: (a) Numerical results of the sample entropy (the red curve) and the KS entropy (the black curve) as a function of the injection strength  $\kappa_{inj}$ . (b) Correlation plot between the sample entropy and the KS entropy shown in Fig. 5(a).

#### 6. Comparison between the $(\epsilon, \tau)$ entropy and the sample entropy

In this section, we investigate the sample entropy and the  $(\epsilon, \tau)$  entropy, which are compared with the KS entropy. Figure 6 shows the cross-correlation values between the sample entropy and the KS entropy, and between the  $(\epsilon, \tau)$  entropy and the KS entropy, as a function of the data length  $N$ . As the data length  $N$  is decreased, the correlation values decrease for the  $(\epsilon, \tau)$  entropy. However, high correlation values are maintained for the sample entropy for small  $N$ . When the data length is set to  $10^4$  points, the correlation values between the sample entropy and the KS entropy is 0.948, and the correlation value between the  $(\epsilon, \tau)$  entropy and the KS entropy is 0.591. Therefore, we can estimate

the entropy accurately using the sample entropy with a shorter data length  $N$  than that for the  $(\epsilon, \tau)$  entropy.

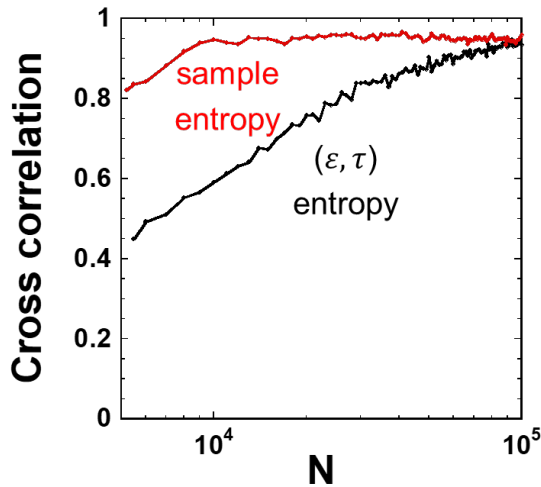


Figure 6: Cross-correlation values between the sample entropy and the KS entropy (the red curve), and between the  $(\epsilon, \tau)$  entropy and the KS entropy (the black curve) as a function of the data length  $N$ .

## 7. Conclusions

We calculated the sample entropy from the temporal waveforms of the optical intensity in unidirectionally coupled semiconductor lasers in numerical simulation. We compared the sample entropy with the KS entropy, which was calculated from the linearized equations of the original model equations for the semiconductor lasers, and showed the validity of the calculation of the sample entropy. We also calculated the correlation between the sample entropy and the KS entropy, and between the  $(\epsilon, \tau)$  entropy and the KS entropy. We found that the sample entropy can be calculated more precisely with shorter data length than that for the  $(\epsilon, \tau)$  entropy.

## Acknowledgments

This work was supported in part by JSPS KAKENHI (JP19H00868 and JP20K15185), JST CREST JPMJCR17N2, and The Telecommunications Advancement Foundation.

## References

[1] A. Uchida, K. Amano, M. Inoue, K. Hirano, S. Naito, H. Someya, I. Oowada, T. Kurashige, M. Shiki, S. Yoshimori, K. Yoshimura, and P. Davis, "Fast physical random bit generation with chaotic semiconductor lasers," *Nature Photonics*, Vol. 2, No. 12, pp. 728 (2008).

[2] I. Kanter, Y. Aviad, I. Reidler, E. Cohen, and M. Rosenbluh "An optical ultrafast random bit generator," *Nature Photonics*, Vol. 4, No. 1, pp. 58 (2010).

[3] Y. Akizawa, T. Yamasaki, A. Uchida, T. Harayama, S. Sunada, K. Arai, K. Yoshimura, and P. Davis, "Fast Random number generation with bandwidth-enhanced chaotic semiconductor lasers 8×50 Gb/s," *IEEE Photonics Technology Letters*, Vol. 24, No. 12, pp. 1042 (2012).

[4] R. Sakuraba, K. Iwakawa, K. Kanno, and A. Uchida, "Tb/s physical random bit generation with bandwidth-enhanced chaos in three-cascaded semiconductor lasers," *Optics Express*, Vol. 23, No. 2, pp. 1470 (2015).

[5] J. D. Hart, Y. Terashima, A. Uchida, G. B. Baumgartner, T. E. Murphy, and R. Roy, "Recommendations and illustrations for the evaluation of photonic random number generators," *APL Photonics*, Vol. 2, pp. 090901 (2017).

[6] J. P. Eckmann and D. Ruelle, "Ergodic theory of chaos and strange attractors," *Reviews of Modern Physics*, Vol. 57, pp. 617 (1985).

[7] P. Gaspard and X. J. Wang, "Noise, chaos, and  $(\epsilon, \tau)$  entropy per unit time," *Physics Reports*, Vol. 235, No. 6, pp. 291 (1993).

[8] A. Cohen and I. Procaccia, "Computing the Kolmogorov entropy from time signals of dissipative and conservative dynamical systems," *Physical Review A*, Vol. 31, No. 3, pp. 1872 (1985).

[9] J. S. Richman and J. R. Moorman "Physiological time-series analysis using approximate entropy and sample entropy," *American Journal of Physiology. Heart and Circulatory Physiology* Vol.278, No.6, pp 2039 (2000).

[10] D. E. Lake, J. S. Richman, M. P. Griffin, and J. R. Moorman, "Sample entropy analysis of neonatal heart rate variability," *American Journal of Physiology-Regulatory, Integrative and Comparative Physiology*, Vol. 283 No. 3, pp. 789 (2002).

[11] R. Lang and K. Kobayashi, "External optical feedback effects on semiconductor injection laser properties," *IEEE Journal of Quantum Electronics*, Vol. 16, No. 3, pp. 347 (1980).

[12] K. Kanno and A. Uchida, "Consistency and complexity in coupled semiconductor lasers with time-delayed optical feedback," *Physical Review E*, Vol. 86, pp. 066202 (2012).